ON THE REACTION OF HEXACHLOROCYCLOTRIPHOSPHAZENE WITH HEPTAMETHYLDISILAZANE. CRYSTAL STRUCTURE OF $P_3N_3Cl_5\{N(CH_3)[Si(CH_3)_3]\}$

Radka VOZNICOVÁ[a1], Milan ALBERTI[b], Jan TARABA[a2], Dalibor DASTYCH[a3], Pavel KUBÁČEK[a4] and Jiří PŘÍHODA[a5,*]

[a] *Department of Chemistry, Faculty of Science, Masaryk University, Kotlářská 2, 611 37 Brno, Czech Republic; e-mail: [1] voznic@post.cz, [2] taraba@chemi.muni.cz, [3] dastych@chemi.muni.cz, [4] kubacek@chemi.muni.cz, [5] prihoda@chemi.muni.cz*

[b] *Department of Physical Electronics, Masaryk University, Kotlářská 2, 611 37 Brno, Czech Republic; e-mail: alberti@chemi.muni.cz*

Received February 27, 2007
Accepted August 15, 2007

The reaction of $P_3N_3Cl_6$ (**1**) with heptamethyldisilazane in the molar ratio 1:1 leads to the formation of 2,4,4,6,6-pentachloro-*N*-methyl-*N*-(trimethylsilyl)cyclotriphosphazen-2-amine, $P_3N_3Cl_5\{N(CH_3)[Si(CH_3)_3]\}$ (**2**). Compound **2** was characterized by elemental analysis and spectroscopically. Molecular and crystal structures of **2** were determined by X-ray diffraction. **2** is monoclinic, space group $P2_1/n$. Experimental data were compared with results of DFT calculations.

Keywords: Phosphazenes; Cyclotriphosphazene; X-ray diffraction; IR spectroscopy; Raman spectroscopy.

The chemistry of phosphazenes was extensively studied in the last 40 years. The research was carried out in the field of preparation and reactivity of linear as well as cyclic phosphazenes with the aim to prepare suitable precursors for syntheses of phosphazene polymers. Detailed information on the present state of art in this field can be found in monographs[1,2].

A common reaction of phosphazenes is the nucleophilic substitution of halogen atoms. These reactions were mostly studied with hexahalogenocyclotriphosphazene $P_3N_3X_6$ (X = F, Cl, Br)[1], their ammonolysis and aminolysis being the most significant reaction types. The extent of the substitution depends on the amine, type of solvent, etc. The results of these studies were summarized in refs[1,3,4].

So far, relatively little attention has been paid to reactions of cyclic phosphazenes with silylated amines. The reactions of $P_3N_3Cl_6$ (**1**) and some amidophosphazenes with hexamethyldisilazane (HMDSN) were studied by

doi:10.1135/cccc20071407

some authors[5–7]. However, only the results of Fields and Allen[7] can be considered as correct. They isolated and characterized a geminal derivative $P_3N_3Cl_4[NHSi(CH_3)_3]_2$ that was formed in the reaction of $P_3N_3Cl_4(NH_2)_2$ with HMDSN in the absence of solvent. Latter Allen and Brown completed this work by publishing spectroscopic data for this compound and determining its crystal and molecular structures[8]. Niecke et al.[9] synthesized partly silylated fluorocyclotriphosphazenes, $P_3N_3F_5[NHSi(CH_3)_3]$, $P_3N_3F_5\{N(CH_3)[Si(CH_3)_3]\}$, $P_3N_3F_5\{N[Si(CH_3)_3]_2\}$ and $P_3N_3F_5\{N(C_2H_5)[Si(CH_3)_3]\}$, by the reaction of aminopentafluorocyclotriphosphazene or the corresponding *N*-alkylated derivatives with $(C_2H_5)_2NSi(CH_3)_3$. All these products were fully characterized by IR and NMR spectroscopies, mass spectrometry, and elemental analysis. Recently, three novel silylamino derivatives, i.e. $P_3N_3Cl_5[NHSi(CH_3)_3]$, $P_3N_3Cl_2[NHSi(CH_3)_3]_4$ and $P_3N_3Cl_2(NH_2)_2[NHSi(CH_3)_3]_2$, were prepared and characterized[10].

This paper deals with the reaction of $P_3N_3Cl_6$ with heptamethyldisilazane (HPMDSN). This reaction has not been studied till now and its proposed course is shown in Scheme 1.

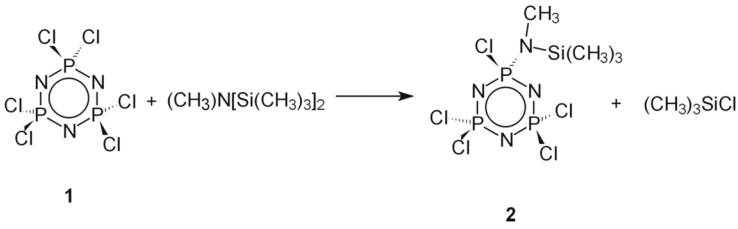

1 **2**

SCHEME 1

EXPERIMENTAL

All procedures, syntheses and sample preparations were performed using Schlenk technique under dry nitrogen atmosphere. Acetonitrile, dichloromethane, diethyl ether and *n*-hexane (Aldrich, p.a.) were purified and dried according to procedures described by Perrin and Armarego[11].

The pure hexachlorocyclotriphosphazene (**1**) was obtained from its mixture with octachlorocyclotetraphosphazene (BASF) by crystallization from *n*-hexane and subsequent sublimation in vacuum at 60 °C. The purity of **1** was determined by mass spectrometry and ^{31}P NMR spectroscopy. HPMDSN (Aldrich, p.a.) was dried by storing over molecular sieve (3 Å) for one week, and then distilling on a Vigreux column. The fraction boiling at 144.0–145.5 °C was collected and the purity of the product was proved by Raman spectroscopy.

^1H, ^{13}C and ^{31}P NMR spectra (δ, ppm; *J*, Hz) were recorded using a Bruker Avance DRX 500 instrument at frequencies ^1H: 500.13 MHz, ^{13}C: 125.77 MHz, ^{31}P: 202.46 MHz, and were referenced to tetramethylsilane and 85% solution of H_3PO_4 (external standard). The samples were sealed in Simax® tubes (diameter 4 mm), inserted in original Wilmad® NMR cuvettes

(diameter 5 mm) and the space between the cuvettes was filled with D_2O (external lock). The spectra were measured in the coaxial NMR cuvette system.

IR spectra (wavelengths in cm^{-1}) were measured with a Bruker IFS 28 spectrometer in KBr disks containing 1.0–1.7 mg of the sample and 100 mg KBr. Raman spectra (in cm^{-1}) of solid samples were measured in Raman capillaries using a Bruker IFS 55 Equinox apparatus, equipped with a FRA 106/S adapter (Nd:YAG laser, λ = 1064 nm, output 150–400 mW).

Diffraction data were collected using the KUMA KM-4 κ-axis diffractometer with graphite-monochromatized MoKα radiation (λ = 0.71073 Å) equipped with a CCD detector. All structures were solved by direct methods, and refined by full-matrix least-squares methods using anisotropic thermal parameters for the non-hydrogen atoms. The software Xcalibur CCD system[12] was used for data collection/reduction, and the SHELXTL software[13] was used for the structure solution, refinement, and drawing preparation (thermal ellipsoids are drawn at the 50 probability level).

Mass spectra were measured using the MAT Trio 1000, Series II, Finnigan, excitation energy 70 eV, connected to a gas chromatograph GC 8000 with DB-5 column. The sample (1–2 μl) in a suitable solvent was injected onto the column, the temperature of the heated zone was 50–280 °C, and the heating rate 10 °C/min. Nitrogen was used as a carrier gas.

Thermal behavior was investigated with a Derivatograph (MOM, Budapest). The TG, DTG, and DTA curves were determined in air up to 900 °C with a heating rate of 2 or 10 °C/min.

The quantum chemical calculations were carried out with the molecular ADF code, version 2005.01 (refs[14–16]), using XC functional LDA including VWN correlation functional, TZ2P basis set and no frozen core.

Synthesis of 2,4,4,6,6-Pentachloro-*N*-methyl-*N*-(trimethylsilyl)-cyclotriphosphazen-2-amine (**2**)

Hexachlorocyclotriphosphazene (**1**; 2.548 g, 7.3 mmol), acetonitrile (13 cm^3) and HPMDSN (1.350 g, 7.7 mmol, 1.7 cm^3, 5% excess) were placed into a Schlenk tube equipped with a screw cap. The reaction mixture was heated on an oil bath at 126–132 °C for 16 h. After cooling, the solvent was partly evaporated and crystals were filtered off with a Schlenk frit S4. The last residue of acetonitrile was removed in vacuum and the product was purified by vacuum sublimation at 70 °C. Yield 1.792 g, 60%. M.p. 92–93 °C. For $P_3N_3Cl_5\{N(CH_3)[Si(CH_3)_3]\}$ (386.4) calculated: 11.59% C, 2.92% H, 42.77% Cl, 13.52% N, 22.42% P, 6.78% Si; found: 11.78% C, 2.92% H, 42.63% Cl, 13.40% N, 22.29% P, 6.37% Si. IR (KBr): 410 sh, 417 w, 500 sh, 514 st, 523 m, 533 sh, 552 w, 565 w, 582 vst, 647 w, 669 w, 693 vw, 764 sh, 769 m, 848 st, 862 sh, 868 sh, 882 w, 953 st, 1069 m, 1191 vst, 1199 sh, 1231 st, 1242 sh, 1257 m, 1264 sh, 1417 vw, 1436 vw, 1458 vw, 1464 vw, 2832 vw, 2900 vw, 2942 sh, 2962 vw, 2972 sh, 2981 sh, 2992 sh. Raman (capillary): 130 vw, 163 m, 177 s, 186 w, 204 m, 214 w, 235 vw, 246 vw, 279 vw, 333 w, 343 m, 356 s, 366 m, 408 s, 518 vw, 532 vw, 556 bvw, 579 vw, 647 vs, 669 w, 693 vw, 769 m, 847 vw, 956 vw, 1067 vw, 1210 vw, 1126 vw, 1265 vw, 1415 vw, 1435 vw, 2832 vw, 2902 s, 2960 m, 2971 sh, 2983 w. MS (EI), *m/z* (rel.%): *M*(theor.) = 414.437 or 411.849 with respect to isotopic composition; 412 (17) $[M^+]$, 397 (100) $[M^+ - CH_3]$, 377 (15) $[M^+ - Cl]$, 339 (7) $[M^+ - Si(CH_3)_3]$, 325 (9) $[M^+ - Si(CH_3)_4]$, 311 (28), 305 (25) $[M^+ - ClSi(CH_3)_3]$, 276 (73) $[M^+ - ClNSi(CH_3)_4]$, 269 (7) $[M^+ - Cl_2Si(CH_3)_3]$, 254 (40) $[M^+ - Cl_2Si(CH_3)_4]$, 240 (40) $[M^+ - Cl_2NSi(CH_3)_4]$, 219 (8) $[M^+ - Cl_3Si(CH_3)_4]$, 206 (9) $[M^+ - Cl_3NSi(CH_3)_4]$, 161 (12) $[M^+ - Cl_5NSi(CH_3)_4]$, 146 (22), 112 (20), 102 (77) $[NSi(CH_3)_4^+]$, 73 (75) $[Si(CH_3)_3^+]$, 59 (69). ^1H NMR (CH_2Cl_2): 2.8 d (NCH_3);

0.37 s ($SiCH_3$), J_{PH} = 15. ^{13}C NMR (CH_2Cl_2): 30.22 s (NCH_3); 0.29 s ($SiCH_3$). $^{31}P\{^1H\}$ NMR (CH_2Cl_2): 22.3 dd (ClP{$N(CH_3)[Si(CH_3)_3]$}); 21.4 d (PCl_2), $^2J_{PP}$ = 50; 21.4 d (PCl_2), $^2J_{PP}$ = 41.

RESULTS AND DISCUSSION

Compound **2** is poorly soluble in acetonitrile (2.3 g/100 cm^3) and therefore this solvent can be used for recrystallization. The solubilities of **2** in diethyl ether and dichloromethane are higher (10 g/100 cm^3). Compound **2** is relatively stable in air, which was proved by IR and Raman spectra. The IR and Raman spectra of **2**, exposed to air moisture for one week, remained unchanged, as confirmed by comparison with IR and Raman spectra of the sample that was kept dry in a Schlenk vessel.

The ^1H, ^{13}C and ^{31}P NMR spectra of **2** were recorded in dichloromethane. The character of the ^{31}P and $^{31}P\{^1H\}$ NMR spectra (Fig. 1a, 1b) at 303 K corresponds to the substitution of one chlorine atom in **1** (refs[10,17]).

It follows from the structure of **2** that $^{31}P\{^1H\}$ NMR spectrum (Fig. 1a) should be of ABC spin system. Doublet of doublets at 22.3 ppm ($^2J_{PP}$ values found in spectrum are 41 and 50 Hz) belongs to the phosphorus atom in $P(Cl)[N(CH_3)_3Si(CH_3)_3]$ group. Two other doublets at 21.4 ppm are observed in the remaining part of the spectrum. According to the theory, these signals should be doublet of doublets but chemical shifts of both PCl_2 groups are so near (the difference is only hundredths of ppm) that only doublets are registered.

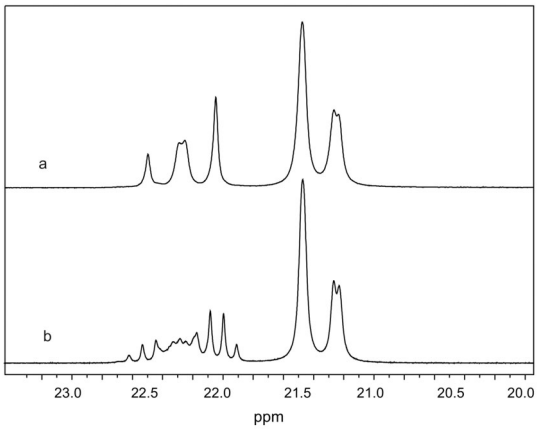

FIG. 1
^{31}P NMR spectra of compound **2**: $\{^1H\}$ decoupled (a), coupled (b)

The coupled ^{31}P NMR spectrum of **2** (Fig. 1b) can be considered as $ABCX_3$ spin system due to the influence of the CH_3 group bonded to exocyclic N-atom ($^3J_{PH}$ = 18 Hz). The shape of the multiplets in the spectra is strongly influenced by a small difference of the chemical shifts of both groups. The interaction of CH_3 protons leads to splitting of each line of the signal at 22.3 ppm, yielding theoretically a quartet. Since these multiplet lines overlap, a broad signal is observed.

The two resonance signals in the ^{13}C NMR spectrum at 30.22 and 0.29 ppm, integral intensity 1:3, prove the presence of two chemically nonequivalent CH_3 groups in **2**, $N(CH_3)$ and $Si(CH_3)_3$. The ^1H NMR spectrum also confirms the proposed structure of **2**.

Figure 2 shows thermal behavior of **2**. It follows from the DTA curve that **2** melts at 92–93 °C. Further heating led to sublimation of the product. The ability of **2** to sublime was also confirmed in a direct experiment where the total weight loss of the sample was observed above 120 °C.

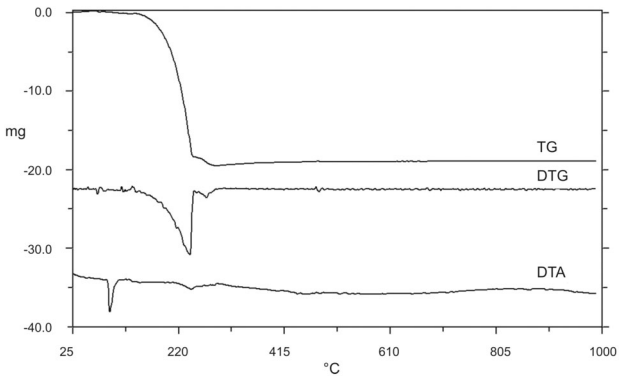

FIG. 2
Thermal behavior of compound **2**

Vibrational Spectra

The measured and calculated IR and Raman spectra are shown in Fig. 3.

The presence of the $CH_3NSi(CH_3)_3$ group in $P_3N_3Cl_5\{N(CH_3)[Si(CH_3)_3]\}$ (**2**) affects the bands in three regions:

a) Antisymmetrical (υ_{as}) and symmetrical vibrations (υ_s) valence bands of CH_3 groups (in trimethylsilyl and methylamino groups) can commonly be found in the region 2800–3000 cm^{-1} (refs[18,19]). These bands are broader and

have weak intensity in the IR spectrum (agreement with N(4)–CH_3 vibration at 2946 cm^{-1} in the simulated spectrum), while in Raman spectrum sharp intensive lines at 2960 (m) and 2902 (s–vs) cm^{-1} together with other less intensive bands are observed[19]. The substitution of Cl atom in $P_3N_3Cl_6$ by $CH_3NSi(CH_3)_3$ group leads to lower symmetry ($D_{3h} \rightarrow C_s$). This change is documented by the presence of more lines in vibration spectrum of **2** complemented with combination lines of weaker intensities and higher harmonic bands (overtones), e.g. 2 × $\delta_{as}CH_3$ (ref.[18]).

b) Bands in the 1200–1500 cm^{-1} region arise by deformation vibrations δ_{as} and δ_s of CH_3 groups of the above mentioned substituent. δ_{as}Si–CH_3 and δ_{as}N(4)–CH_3 bands in the 1464–1368 cm^{-1} region in IR spectrum, and in the 1468–1375 cm^{-1} region in Raman spectrum (Fig. 3) are unresolved, with numerous overlaps. The intensive band at 1231 cm^{-1} together with a shoulder

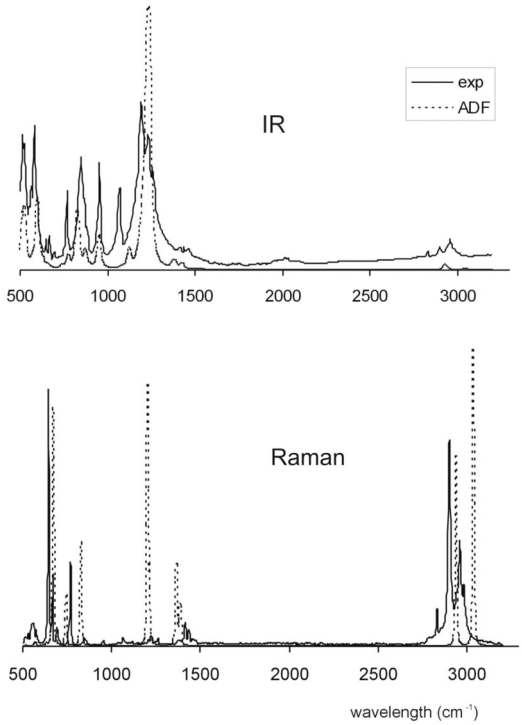

FIG. 3
Measured and calculated IR and Raman spectra of compound **2**

at 1242 cm^{-1} in the IR experimental spectrum can be assigned to δ_s vibrations of both types of CH_3 groups, while the same bands are less intensive in Raman spectrum (Fig. 3). The corresponding band at 1206 cm^{-1} for CH_3 from the Si–CH_3 group was found in simulated IR spectrum. These observations are also in agreement with published data[19,20].

It is worthwhile to mention the bands of symmetrical valence vibrations υ of endocyclic P and N atoms of compound **2**. These bands, at 1257 (st) cm^{-1} and the shoulder 1264 (m) cm^{-1}, are of negligible intensity in Raman spectrum, but very intensive in IR spectrum. These can be compared with two intensive bands at 1234 and 1257 cm^{-1} in simulated IR spectrum and literature data as well[7,19,21–23].

The most intensive band in IR spectrum is at 1191 cm^{-1}, with a shoulder at 1199 cm^{-1}. According to the ADF program, this band arises by the combination of valence vibration υ_{as} of exocyclic P(1)–N(4) bond or υ_{as}P(1)–N(4)–C(4) (theoretically 1186 cm^{-1}), and υSi–N(4)–C(4). Shihada[24] assigned the band at 1115 cm^{-1} in IR spectrum, and the corresponding band at 1124 cm^{-1} in Raman spectrum of the compound $Cl_2PONHCH_3$ just to the υ_{as}P–N–C vibration. Similarly, the band of medium intensity at 1069 cm^{-1} (1080 cm^{-1} in simulated ADF spectrum) can be assigned to υN(4)–C(4) or υSi–N(4)–C(4) valence vibrations. The corresponding values were found in $CH_3N[Si(CH_3)_3]_2$ (ref.[20]). Another proof of substitution comes from the band at 953 cm^{-1} (954 cm^{-1} in simulated spectrum) corresponding to the vibration of exocyclic P(1)–N(4) bond.

c) Further bands, providing information about substitution in **2**, can be found in the 600–900 cm^{-1} region. They can be assigned either to $\rho_{as}(CH_3)$ and $\rho_s(CH_3)$ deformation vibrations, or $\upsilon_{as}SiC_3$, υ_sSiC_3, and υSi–N–C_3 valence vibrations. The band observed at 848 cm^{-1} in IR spectrum (847 (vw) cm^{-1} in Raman spectrum; 835 cm^{-1} in ADF spectrum) can be unambiguously assigned to $\rho_{as}(CH_3)$ deformation vibration[18–20]. Bands at 882 (w), 868 (sh), 862 (sh), 831, 823, and 821 cm^{-1} in ADF spectrum) correspond to υSiC_3 valence vibrations.

According to literature data[18], it is possible to assign the 769 cm^{-1} band of low or medium intensity in IR spectrum (also 769 cm^{-1} in Raman spectrum) to $\rho_s(CH_3)$ deformation vibration. The very intensive band at 647 cm^{-1} in Raman spectrum is due to υ_sSiC_3 valence vibration, while the low intensity bands at 669 cm^{-1} (Raman) and 669, 647 cm^{-1} (IR) can be assigned to $\upsilon_{as}SiC_3$ valence vibration[18,20].

The spectra calculated on the used level of DF theory have been useful in the assigning experimental bands to a mode of vibratory motion, however not in every case. The molecule has no symmetry and is too big for higher

level of precise calculation. Moreover, its stereochemical nonrigidity is likely to worsen the agreement between theory and experiment.

*The Crystal Structure of 2,4,4,6,6-Pentachloro-N-methyl-N-(trimethylsilyl)cyclotriphosphazen-2-amine (**2**)*

Single crystals of **2** were grown from its concentrated acetonitrile solution at room temperature over a period of few days.

The molecular and crystal structures of **2** were determined by X-ray structure analysis. Compound **2** is monoclinic, space group $P2_1/n$, $Z = 4$ (Fig. 4). The basic crystallographic data are given in Table I and selected bond lengths and angles in Table II. The P_3N_3 ring is slightly deformed, whereas the P(1) atom bearing the $CH_3NSi(CH_3)_3$ group is positioned off the ring plane. The mean deviation of P(1) from the ring plane is 0.2442 Å.

It follows from a comparison of the molecular structure of **2**, $P_3N_3Cl_6$ (ref.[25]) and other monosubstituted cyclophosphazenes that the P(1)–Cl(1) bond in **2** (2.0284 Å) is longer than, e.g., in **1** (1.985 Å), but comparable to other monosubstituted derivatives (2.010–2.046 Å)[26–28]. Other P–Cl bonds in PCl_2 groups of the ring remained unchanged. The N(4)–P(1)–Cl(1) angle is 106.25(7)°.

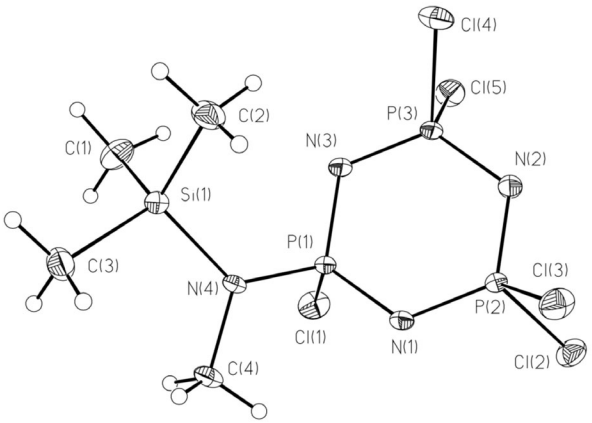

FIG. 4
The molecular structure of compound **2**. The thermal ellipsoids of non-hydrogen atoms are drawn at the 50% probability level

The space crystal structure arrangement (Fig. 5) consists of chains [010] in which the molecules of **2** form the plane (101). The chains with the $[ABAB]_\infty$ motive alternate regularly. No more significant weak interactions were observed.

TABLE I
Crystal data and refinement parameters for compound **2**

Empirical formula	$C_4H_{12}Cl_5N_4P_3Si$
M, g mol^{-1}	414.43
T, K	120
Wavelength, Å	0.71069
Crystal system, space group	monoclinic, $P2(1)/n$
a, Å	15.496(3)
b, Å	6.1260(10)
c, Å	17.734(4)
β, °	109.51(3)
V, Å^3	1586.8(5)
Z	4
Calculated density, Mg m^{-3}	1.735
Absorption coefficient, mm^{-1}	1.276
F(000)	832
Crystal size, mm	0.25 × 0.25 × 0.1
θ range for data collection, °	3.54–25.00
Index ranges	$-20 \le h \le 17$, $-8 \le k \le 7$, $-22 \le l \le 23$
Reflections collected/unique	10940/3645 [R(int) = 0.0843]
Completeness to 2θ = 25.00, %	98.4
Refinement method	Full-matrix least-squares on F^2
Data/restraints/parameters	3645/0/158
Goodness-of-fit on F^2	1.085
Final R indices [$I > 2\sigma(I)$]	R_1 = 0.0359, wR_2 = 0.1001
R indices (all data)	R_1 = 0.0381, wR_2 = 0.1025
Largest diff. peak and hole, e Å^{-3}	0.843 and –0.562

The agreement between the data obtained from X-ray diffraction and from ADF calculation (Table II) can be observed from the average of their difference expressed in per cent, which is 0.7 for internuclear distances (12 values) and 0.8 for angles (25 values). The deformation of the ring into an approximate envelope conformation can be characterized by the angle between two planes: N(1)–P(1)–N(3) and N(1)–N(2)–N(3) (see Fig. 4). This angle amounts to 16° (X-ray data) and 17° (ADF calculation). The molecule **2** could well be stereochemically nonrigid because of the low barrier to rotation around the P(1)–N(4) bond. With all other coordinates optimized

TABLE II
Selected experimental and calculated bond lengths (in Å) and angles (in °) for compound **2**

	X-ray	ADF[a]		X-ray	ADF[a]
	Bond, Å			Angles, °	
P(1)–N(3)	1.585(2)	1.594	P(3)–N(2)–P(2)	119.93(11)	122.2
P(1)–N(1)	1.589(2)	1.596	N(3)–P(1)–N(1)	116.30(9)	116.7
P(1)–N(4)	1.603(2)	1.618	N(3)–P(1)–N(4)	109.80(9)	108.6
P(1)–Cl(1)	2.028(1)	2.045	N(1)–P(1)–N(4)	111.51(9)	111.5
N(1)–P(2)	1.562(2)	1.571	N(3)–P(1)–Cl(1)	107.30(7)	108.0
N(4)–C(4)	1.480(2)	1.456	N(1)–P(1)–Cl(1)	105.00(7)	105.9
N(4)–Si(1)	1.781(2)	1.786	N(4)–P(1)–Cl(1)	106.25(7)	105.5
Si–C[b]	1.847(2)	1.853	P(2)–N(1)–P(1)	121.20(10)	120.3
P(2)–N(2)	1.575(2)	1.585	C(4)–N(4)–P(1)	114.40(14)	115.0
P–Cl[b]	1.991(1)	2.002	C(4)–N(4)–Si(1)	119.59(14)	120.8
N(2)–P(3)	1.571(2)	1.580	P(1)–N(4)–Si(1)	125.65(9)	121.6
P(3)–N(3)	1.568(2)	1.576	C–Si–C[c]	110.33(9)	111.0
	Angles, °		N–Si–C[c]	108.55(9)	107.7
N(1)–P(2)–N(2)	119.48(9)	118.3	N(3)–P(3)–N(2)	119.40(9)	118.5
N(1)–P(2)–Cl(3)	109.21(7)	107.7	N(3)–P(3)–Cl(5)	110.12(7)	110.0
N(2)–P(2)–Cl(3)	108.39(8)	109.2	N(2)–P(3)–Cl(5)	108.13(8)	108.2
N(1)–P(2)–Cl(2)	110.08(7)	110.9	N(3)–P(3)–Cl(4)	108.27(7)	107.8
N(2)–P(2)–Cl(2)	107.57(8)	108.0	N(2)–P(3)–Cl(4)	108.39(8)	109.6
Cl–P–Cl[c]	100.68(3)	101.3	P(3)–N(3)–P(1)	120.61(10)	120.8

[a] All coordinates optimized with TZ2P basis and no frozen core. [b] Average length. [c] Average angle.

except for the changing dihedral angle ξ Cl(1)–P(1)–N(4)–Si, the ADF calculation shows one barrier for ξ = 0° and another for ξ = 180°. The barriers lie at 0.51 and 0.14 eV, respectively, above the minima that occur symmetrically for ξ = 100 and 260°. The whole calculated energy profile is shown in Fig. 6.

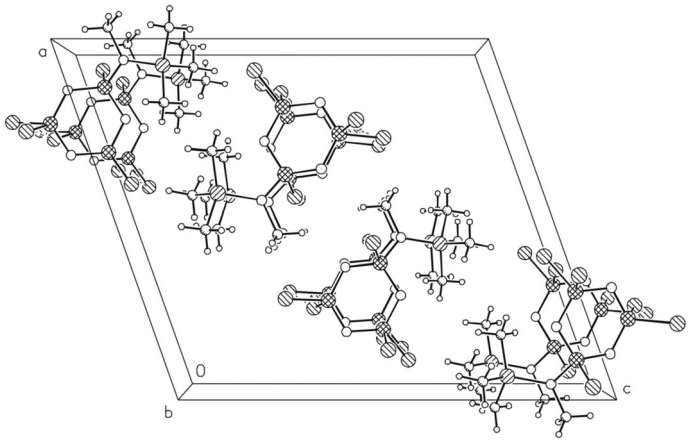

FIG. 5
The crystal structure – perspective view through molecular composition of compound **2**

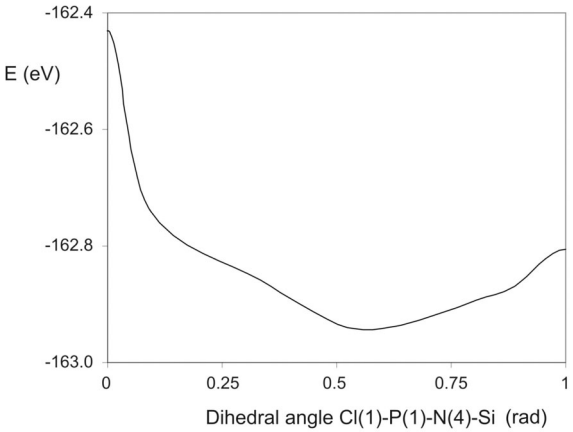

FIG. 6
Calculated energy profile for internal rotation of the $CH_3NSi(CH_3)_3$ group

CCDC 294469 contains the supplementary crystallographic data for this paper. These data can be obtained free of charge via www.ccdc.cam.ac.uk/conts/retrieving.html (or from the Cambridge Crystallographic Data Centre, 12, Union Road, Cambridge, CB2 1EZ, UK; fax: +44 1223 336033; or deposit@ccdc.cam.ac.uk).

This work was supported by the Ministry of Education, Youth and Sports of the Czech Republic (project MSM0021622411). The authors express their gratitude to the Grant Agency of the Czech Republic (grant No. 203/02/0436).

REFERENCES

1. Gleria M., De Jaeger R.: *Phosphazenes, A Worldwide Insight*. Nova Science Publishers, Inc., New York 2002.
2. Allcock H. R.: *Chemistry and Applications of Polyphosphazenes*. Wiley–Interscience, Hoboken and New York 2003.
3. Allen C. W.: *The Chemistry of Inorganic Homo- and Heterocycles* (I. Haiduc and D. B. Sowerby, Eds). Academic Press, London 1987.
4. Allen C. W.: *Chem. Rev.* **1991**, *91*, 119.
5. Mattogno G., Tarli F.: *Ric. Sci. Rend. A* **1964**, *34*, 487.
6. Mattogno G., Monaci A., Tarli F.: *Ann. Chim. (Rome)* **1965**, *55*, 599.
7. Fields A. T., Allen C. W.: *J. Inorg. Nucl. Chem.* **1974**, *36*, 1929.
8. Allen C. W., Brown D. E.: *J. Chem. Soc., Dalton Trans.* **1988**, 1405.
9. Niecke E., Thamm H., Flaskerud G.: *Chem. Ber.* **1971**, *104*, 3729.
10. Jančík V., Alberti M., Taraba J., Žák Z., Herbst-Irmer R., Alexopoulos E.: *Polyhedron*, in press.
11. Perrin D. D., Armagedo W. L. F.: *Purification of Laboratory Chemicals*, 3rd ed. Pergamon Press, Oxford 1988.
12. *Xcalibur CCD System, CrysAlis Software System*, Version 1.168. Oxford Diffraction Ltd., Oxford 2001.
13. *SHELXTL*, Version 5.10. Bruker AXS Inc., Madison (WI) 1997.
14. te Velde G., Bickelhaupt F. M., van Gisbergen S. J. A., Fonseca Guerra C., Baerends E. J., Snijders J. G., Ziegler T.: *J. Comput. Chem.* **2001**, *22*, 931.
15. Guerra C. F., Snijders J. G., te Velde G., Baerends E. J.: *Theor. Chem. Acc.* **1998**, *99*, 391.
16. *ADF 2005.01*, *SCM*, Theoretical Chemistry. Vrije Universiteit, Amsterdam; http://www.scm.com.
17. Alberti M., Břínek J., Marek J., Toužín J.: *Z. Anorg. Allg. Chem.* **1997**, *623*, 637.
18. Bürger H.: *Organomet. Chem.* **1968**, *3*, 425.
19. Guirgis G. A., Horn A., Klaeboe P., Nielsen C. J.: *J. Mol. Struct.* **2006**, *825*, 101.
20. Goubeau J., Jiménez-Barberá J.: *Z. Anorg. Allg. Chem.* **1960**, *303*, 217.
21. Painter P. C., Zarian J., Coleman M. M.: *Appl. Spectrosc.* **1982**, *36*, 265.
22. Huvenne J. P., Vergoten G., Legrand P.: *J. Mol. Struct.* **1980**, *63*, 47.
23. Clare P., Sowerby B. D.: *Spectrochim. Acta* **1981**, *37*, 883.
24. Shihada A. F.: *Z. Anorg. Allg. Chem.* **1975**, *411*, 135.
25. Bullen G. J.: *J. Chem. Soc. A* **1971**, 1450.

26. Bullen G. J.: *J. Crystallogr. Spectrosc. Res.* **1982**, *12*, 11.
27. Allcock H. R., Lavin K. D., Riding G. H., Whittle R. R.: *Organometallics* **1984**, *3*, 663.
28. Babu Y. S., Manohar H., Cameron T. S.: *Acta Crystallogr., Sect. B: Struct. Crystallogr. Cryst. Chem.* **1979**, *35*, 1410.